

Shapes of ${}^3\text{He}$ clusters

Constantine Yannouleas and Uzi Landman

School of Physics, Georgia Institute of Technology, Atlanta, Georgia 30332-0430

(Received 22 February 1996; revised manuscript received 14 May 1996)

Triaxial deformations are considered for determining the binding energies of open-shell, unpolarized ${}^3\text{He}_N$ clusters. The shapes of ${}^3\text{He}$ clusters are found to be close to spherical, in contrast to the well-deformed shapes of alkali-metal clusters. As a result, odd-even alternations and subshell closures between major shells are absent in the size evolution of the chemical potentials, and the second-energy differences associated with ${}^3\text{He}_N$ clusters. [S0163-1829(96)00735-7]

It has been established that a dominant factor controlling the ground-state properties and shapes of disparate finite fermion systems (such as nuclei and simple-metal clusters, whose nature of bonding and cohesion are of very different origins with widely differing characteristic energetic and spatial scales) are the shell effects resulting from level degeneracies in conjunction with the Pauli principle (e.g., for nuclei see Ref. 1; for simple metal clusters see Refs. 2 and 3).

In contrast to heavier noble-gas clusters,^{4,5} where geometrical packing of the atoms controls the stability properties of the ground state, helium atoms remain delocalized within the volume of the cluster, being confined by an average mean-field potential well.⁶ In particular, since ${}^3\text{He}$ obeys fermion statistics, ${}^3\text{He}_N$ clusters may be expected to exhibit certain analogies with atomic nuclei. Indeed, such analogies, pertaining to the short-range character of both the helium-helium and nucleon-nucleon interactions, have motivated the development of theoretical Kohn-Sham-type (KS) density-functional approaches for investigations of ${}^3\text{He}$ clusters.^{6,7} Such density-functional approaches have yielded a wealth of information about several properties of ${}^3\text{He}_N$ clusters. The deformations of open-shell ${}^3\text{He}_N$ clusters, however, have not been included as yet in such treatments.

In this paper, we calculate the shell effects in ${}^3\text{He}_N$ open-shell clusters in conjunction with their equilibrium deformed shapes (the influence of deformation needs to be accounted for, since it is well known that the ground state of both open-shell nuclei¹ and metallic clusters^{2(b),3} does not preserve spherical symmetry). In these calculations, we use a semiempirical shell-correction method (SE-SCM), which accounts for ellipsoidal (triaxial) deformations. This method was introduced³ by us earlier in the context of studies of metal clusters, where it provided a successful interpretation of experimentally observed systematic size-evolutionary patterns of ground-state properties, such as ionization potentials, electron affinities, monomer and dimer separation energies, and fission energetics.

According to the SE-SCM, the total energy of the cluster E_T (usually also denoted^{2(b),3} as E_{sh} to emphasize the fact that shell corrections have been included), is given as the sum of two terms, a liquid-drop-type smooth contribution E_{LD} , and a Strutinsky-type⁸ shell correction, $\Delta E_{\text{sh}}^{\text{Str}}$, namely,

$$E_T = E_{\text{LD}} + \Delta E_{\text{sh}}^{\text{Str}}. \quad (1)$$

The general background⁹ and formulation of this method for the case of neutral and charged simple-metal clusters has been described in Refs. 2(b) and 3. Prior to presenting our results for ${}^3\text{He}$ clusters, we discuss the relevant parameters used in our calculations (as well as other needed modifications).

For a deformed neutral cluster, the liquid-drop model^{2(b),3} (LDM) expresses the *smooth* part E_{LD} of the total energy as the sum of three contributions, namely, a volume, a surface, and a curvature term,

$$E_{\text{LD}} = E_{\text{vol}} + E_{\text{surf}} + E_{\text{curv}} = A_v \int d\tau + \sigma \int dS + A_c \int dS \kappa, \quad (2)$$

where $d\tau$ is the volume element, dS is the surface differential element, and κ is the local curvature of the droplet which models the cluster. In the case of ${}^3\text{He}_N$ clusters, the coefficients of the three contributions have been determined by fitting⁶ the total energy from KS-type calculations for closed-shell, magic spherical clusters (i.e., for $N=20, 40, 70, 112, 168, 240,$ and 330 , which happen to be the magic numbers corresponding to an isotropic harmonic-oscillator central potential) to the following parametrized expression as a function of the number N of atoms in the cluster,

$$E_{\text{LD}}^{\text{sph}} = \alpha_v N + \alpha_s N^{2/3} + \alpha_c N^{1/3} + \alpha_0. \quad (3)$$

The following expressions relate the coefficients A_v , σ , and A_c to the corresponding coefficients, (α 's), in Eq. (3): $A_v = 3\alpha_v / (4\pi r_0^3)$, $\sigma = \alpha_s / (4\pi r_0^2)$, and $A_c = \alpha_c / (4\pi r_0)$, r_0 being the unit radius [see Eq. (7) below]. In Ref. 6, it was found that $\alpha_v = -2.49$ K, $\alpha_s = 8.42$ K, $\alpha_c = 4.09$ K, and $\alpha_0 = -19.8$ K. How to calculate the integrals entering into Eq. (2) in the case of ellipsoidal shapes is described in detail in Sec. II A of Ref. 3.

Since the magic numbers of ${}^3\text{He}_N$ clusters correspond to major closures of an *isotropic* harmonic-oscillator potential,^{6,10} a natural choice for the external model potential to be used for calculating shell corrections in the SE-SCM is an *anisotropic* three-dimensional oscillator,

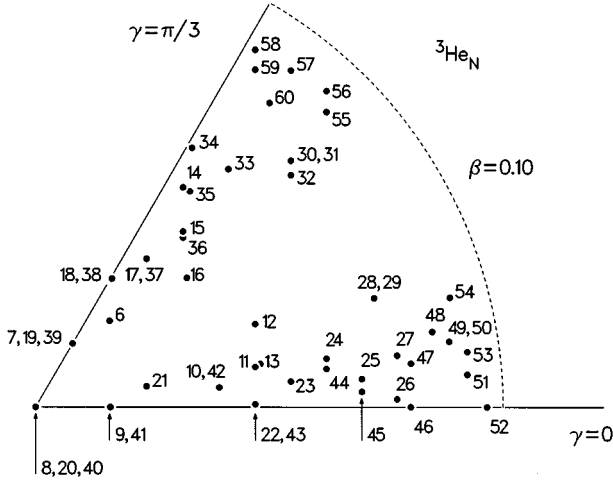


FIG. 1. The Hill-Wheeler parameters specifying the equilibrium shapes (corresponding to the global minima of the PES's) of ${}^3\text{He}_N$ clusters according to the ellipsoidal model in the range $6 \leq N \leq 60$. Observe that the dashed circle corresponds to a value of $\beta = 0.10$, compared to a much larger value of $\beta = 0.70$ for Na clusters (see Fig. 22 in Ref. 3).

$$H_0 = -\frac{\hbar^2}{2m^*} \Delta + \frac{m^*}{2} (\omega_1^2 x^2 + \omega_2^2 y^2 + \omega_3^2 z^2). \quad (4)$$

The oscillator frequencies can be related to the principal semiaxes a' , b' , and c' of the ellipsoid via the volume-conservation constraint, and the requirement that the surface of the cluster is an equipotential one, namely,

$$\omega_1 a' = \omega_2 b' = \omega_3 c' = \omega_0 R_0, \quad (5)$$

where the frequency ω_0 for the spherical shape (with radius R_0) was taken according to Ref. 11 to be

$$\hbar \omega_0(N) = \frac{\hbar^2}{m^* r_0^2} \frac{5}{4} 3^{1/3} N^{-1/3} = \frac{14.46}{r_0^2} N^{-1/3} \text{ K } \text{\AA}^2, \quad (6)$$

where $R_0 = r_0 N^{1/3}$. The effective mass is twice the bare ${}^3\text{He}$ mass,¹¹ i.e., $m^* = 2m$. The unit radius r_0 is a slowly varying function¹² of N , namely,

$$r_0(N) = 2.44 + 12.66N^{-2/3} - 0.23N^{-1/3} \text{ \AA}. \quad (7)$$

The single-particle energies ε_i of the anisotropic harmonic Hamiltonian (4) are used to obtain (as described in detail in Sec. II C of Ref. 3) the semiempirical Strutinsky shell correction $\Delta E_{\text{sh}}^{\text{Str}}$, namely,

$$\Delta E_{\text{sh}}^{\text{Str}} = \sum_i^{\text{occ}} \varepsilon_i - \tilde{E}_{\text{sp}}, \quad (8)$$

where \tilde{E}_{sp} is the Strutinsky average of the single-particle spectrum.

Systematics of the equilibrium triaxial shapes of ${}^3\text{He}_N$ clusters in the range $N \leq 60$ are shown in Fig. 1. These re-

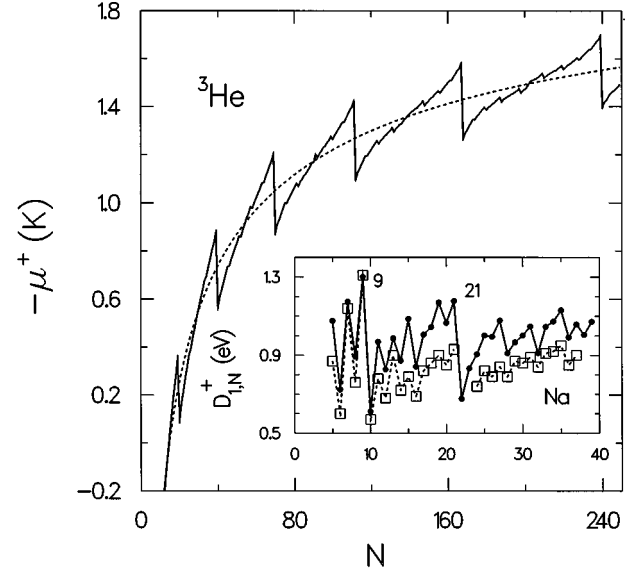


FIG. 2. Theoretical results for the chemical potential $-\mu^+$, of ${}^3\text{He}_N$ clusters. Solid line: SE-SCM results with triaxial deformations. Shell closures occur at $N = 20, 40, 70, 112, 168,$ and 240 . Dashed line: Liquid drop results for corresponding spherical shapes. Energies in units of degrees K. Inset: Monomer separation energies $D_{1,N}^+$ for singly charged, cationic Na_N^+ clusters in the range $5 \leq N \leq 39$. Solid dots: Theoretical results derived from the SE-SCM method with triaxial deformations. Open squares: Experimental measurements from Ref. 15. Energies are in units of eV.

sults are presented using the Hill-Wheeler parameters¹³ β and γ , which are related to the semiaxes of the ellipsoid as follows:

$$a' = R_0 \exp \left[\sqrt{5/(4\pi)} \beta \cos \left(\gamma - \frac{2\pi}{3} \right) \right],$$

$$b' = R_0 \exp \left[\sqrt{5/(4\pi)} \beta \cos \left(\gamma + \frac{2\pi}{3} \right) \right], \quad (9)$$

$$c' = R_0 \exp \left[\sqrt{5/(4\pi)} \beta \cos \gamma \right],$$

where β is unrestricted, and $0 \leq \gamma \leq \pi/3$. A value $\gamma \neq 0$ indicates a triaxial shape, while $\gamma = 0$ corresponds to a prolate shape, and $\gamma = \pi/3$ denotes an oblate deformation. The parameter β provides a measure of the magnitude of the deformation (the origin, i.e., $\beta = 0$, corresponds to a spherical shape).

Using Hill-Wheeler parameters, the cluster potential-energy surfaces (PES's) $E_T(\beta, \gamma; N)$ in deformation space may be easily mapped and studied. In this manner, one can analyze the topography of the PES's and identify the global minimum $E_T(N)$ and the corresponding β and γ for each size N . The equilibrium deformations associated with the global minima are plotted in Fig. 1 for the case of ${}^3\text{He}$.

We observe that although the γ parameter takes values between 0 and $\pi/3$ in the case of ${}^3\text{He}$ clusters, the β parameter exhibits values noticeably smaller than corresponding

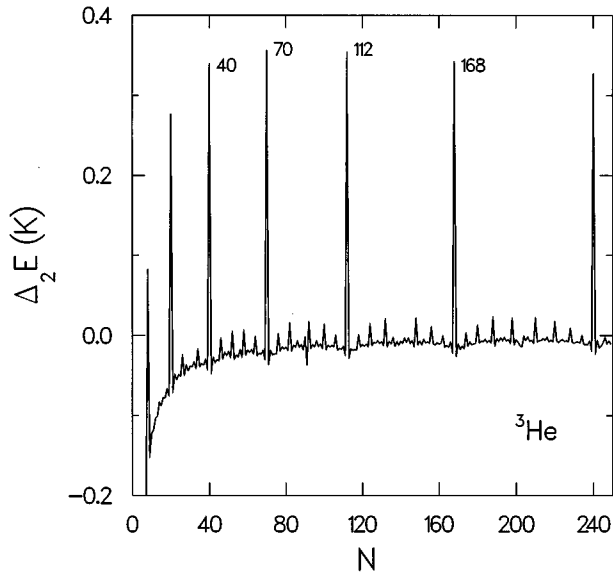


FIG. 3. Theoretical second-energy differences $\Delta_2 E$, for ${}^3\text{He}_N$ clusters derived from the SE-SCM method with triaxial deformations. Energies are in units of degrees K.

values for Na clusters (see Fig. 22 in Ref. 3). As a result, the shapes of ${}^3\text{He}_N$ clusters are much less deformed than those of Na_N clusters. These differences in equilibrium shapes result in marked differences in the various size-evolutionary patterns of ${}^3\text{He}$ and alkali-metal clusters (as was the case with previous investigations,⁶ we find that ${}^3\text{He}$ clusters with $15 \leq N \leq 30$ are metastable, namely, they have $E_T > 0$ and $\mu^+ < 0$. ${}^3\text{He}$ clusters with $N \leq 14$ are unstable, i.e., they have $E_T > 0$ and $\mu^+ > 0$).

Figure 2 displays the size evolution of the chemical potential, $\mu^+ = E_T(N+1) - E_T(N)$ (solid line), of ${}^3\text{He}$ clusters, along with the liquid drop contribution (dashed line). Apart from the prominent features at major-shell closures, the fine structure in between is practically insignificant. This behavior is characteristic of spherical fermionic clusters¹⁴ and correlates with the weak deformation of ${}^3\text{He}$ clusters.

In contrast, the monomer separation energies $D_{1,N}^+ = E_T^+(N-1) - E_T^+(N) + E_T(1)$ associated with the process $\text{Na}_N^+ \rightarrow \text{Na}_{N-1}^+ + \text{Na}$ in the case of singly charged clusters exhibit a rich fine structure between major-shell closures. This behavior, which is a consequence of the significant deformations of Na_N clusters, is displayed in the inset of Fig. 2, where theoretical results are confronted with experimental measurements.¹⁵ In addition to features associated with major-shell closures (i.e., for $N=9$ and 21), odd-even oscillations and subshell closures at $N=15, 27, 31,$ and 35 are prominent.

Another quantity which reflects shell effects in fermion microsystems is the second-energy difference $\Delta_2 E = E_T(N+1) + E_T(N-1) - 2E_T(N)$. For the case of ${}^3\text{He}$ clusters, this quantity is displayed in Fig. 3. Again, as was the case with the chemical potential, only the features at major-shell closures are important.

The second-energy differences for the case of singly charged Na_N^+ clusters are displayed in Fig. 4 (solid line) and compared to experimental results (open squares)

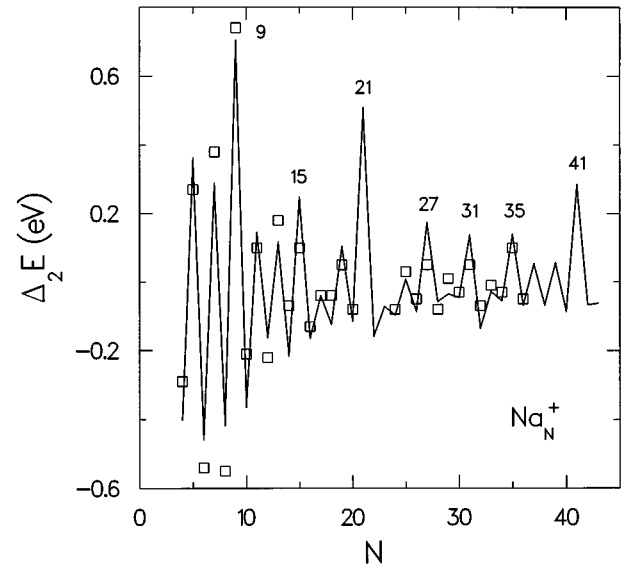


FIG. 4. Second-energy differences $\Delta_2 E$ for singly charged, cationic Na_N^+ clusters. Solid line: Theoretical results derived from the SE-SCM method with triaxial deformations. Open squares: Experimental results extracted from Ref. 15. Energies are in units of eV.

extracted¹⁶ from the measurements of Ref. 15. In contrast to ${}^3\text{He}$ clusters, the importance of fine structure between magic numbers is immediately noticeable. The fine structure between magic numbers, namely, all the odd-even alternations and their modulations (i.e., the attenuation in the range $N=16-19$ or the enhancements at the subshell closures $N=15, 27, 31,$ and 35) apparent in the experimental results are very well reproduced by the theory.

From the above comparisons, we conclude that, even though both ${}^3\text{He}$ and Na clusters are fermionic microsystems, the size-evolutionary patterns of their ground-state properties are substantially different. Underlying the different behaviors of these two systems are the relatively high surface and curvature LDM coefficients of ${}^3\text{He}$ compared to those of Na clusters (for ${}^3\text{He}$ clusters, these coefficients are 8.42 and 4.09 K, respectively; for sodium they are³ 0.541 and 0.154 eV, respectively).

For Na, the effective mass m^* is equal to the bare electron mass m_e and the unit radius r_0 corresponds to the Wigner-Seitz radius $r_s = 4.0$ a.u. If one defines q as the ratio between the surface-energy coefficient and the major-shell energy spacing, namely $q = \alpha_s / (\hbar \omega_0 N^{1/3})$, one finds $q({}^3\text{He}) = 3.47$ (assuming $r_0 = 2.44$ Å), $q(\text{Na}) = 0.18$, and a relative ratio $q({}^3\text{He})/q(\text{Na}) = 19.3$. Thus the weight of the surface energy compared to the weight of the shell correction is about 20 times larger in ${}^3\text{He}$ than it is in the case of Na clusters. This relatively much higher surface energy yields substantially less deformed ${}^3\text{He}$ clusters, and is the reason for the different size-evolutionary patterns between ${}^3\text{He}$ and Na clusters.

This research was supported by the U.S. Department of Energy (Grant No. FG05-86ER-45234). Studies were performed at the Georgia Institute of Technology Center for Computational Materials Science.

- ¹Å. Bohr and B.R. Mottelson, *Nuclear Structure* (Benjamin, Reading, MA, 1975), Vol. II.
- ²For reviews, see (a) W.A. de Heer, *Rev. Mod. Phys.* **65**, 611 (1993); (b) C. Yannouleas and U. Landman, in *Proceedings of the NATO Advanced Study Institute, Course on "Large Clusters of Atoms and Molecules," Erice, Italy, June 1995*, Vol. 313 of *NATO Advanced Study Institute, Series E: Applied Sciences*, edited by T.P. Martin (Kluwer, Dordrecht, 1996), p. 131.
- ³C. Yannouleas and U. Landman, *Phys. Rev. B* **51**, 1902 (1995).
- ⁴See articles by J.P. Toennies, K.B. Whaley, and S. Stringari, in *The Chemical Physics of Atomic and Molecular Clusters, Proceedings of the International School of Physics "Enrico Fermi," 1988*, edited by G. Scoles (North-Holland, Amsterdam, 1990).
- ⁵H. Haberland, in *Clusters of Atoms and Molecules*, edited by H. Haberland, Springer Series in Chemical Physics Vol. 52 (Springer-Verlag, Berlin, 1994), Vol. I, p. 374.
- ⁶S. Stringari and J. Treiner, *J. Chem. Phys.* **87**, 5021 (1987).
- ⁷S. Weisgerber and P.-G. Reinhard, *Z. Phys. D* **23**, 275 (1992).
- ⁸V.M. Strutinsky, *Nucl. Phys. A* **95**, 420 (1967); **122**, 1 (1968).
- ⁹For a microscopic local-density-approximation (LDA) foundation of the shell correction method (LDA-SCM) for metal clusters using the jellium approximation in connection with an extended Thomas-Fermi (ETF) LDA input density to a Harris-like functional, see C. Yannouleas and U. Landman, *Phys. Rev. B* **48**, 8376 (1993). This LDA-SCM has been applied to multiply anionic metal clusters [C. Yannouleas and U. Landman, *Chem. Phys. Lett.* **210**, 437 (1993)] and to multiply charged fullerenes [C. Yannouleas and U. Landman, *Chem. Phys. Lett.* **217**, 175 (1994)]. For an application of our SE-SCM to metal-cluster fission, see C. Yannouleas and U. Landman, *J. Phys. Chem.* **99**, 14 577 (1995); C. Yannouleas, R.N. Barnett, and U. Landman, *Comments At. Mol. Phys.* **31**, 445 (1995).
- ¹⁰A recent Kohn-Sham-type density functional approach (Ref. 7) using finite-range interactions has found that above $N=168$ the shell closures deviate from those of the harmonic oscillator scheme. As was the case for metal clusters, (Ref. 3), in the framework of the SE-SCM these deviations can be taken into account by adding an l^2 perturbation to the Hamiltonian (4). Since, however, in this paper we carry out calculations for smaller, rather than larger, sizes, we will continue our exposition by strictly adopting the harmonic-oscillator magic numbers of Ref. 6. Apart from a rearrangement of magic numbers above 168, our conclusions concerning the contrasting behavior of size-evolutionary patterns of ^3He , and Na clusters will not be affected.
- ¹¹S. Stringari, in *The Chemical Physics of Atomic and Molecular Clusters, Proceedings of the International School of Physics "Enrico Fermi," 1988* (Ref. 4), p. 199.
- ¹²F. Castaño, M. Membrado, A.F. Pacheco, and J. Sañudo, *Phys. Rev. B* **48**, 12 097 (1993).
- ¹³D.L. Hill and J.A. Wheeler, *Phys. Rev.* **89**, 1102 (1953).
- ¹⁴W. Ekardt, *Phys. Rev. B* **29**, 1558 (1984).
- ¹⁵C. Bréchnignac, Ph. Cahuzac, J. Leygnier, and J. Weiner, *J. Chem. Phys.* **90**, 1492 (1989).
- ¹⁶The second-energy differences are immediately calculated from the experimental monomer separation energies listed in Ref. 15 by taking the differences $D_{1,N}^+ - D_{1,N+1}^+$. The experimental value for the monomer separation energy for $N=10$, which was not provided in Ref. 15, was specified with the help of the relation (Ref. 15), $D_{1,11}^+ - D_{2,11}^+ = 0.75 \text{ eV} - D_{1,10}^+$, where $D_{2,N}^+$ denotes the dimer separation energies.